Light Metals 2014
Edited by: John Grandfield
TMS (The Minerals, Metals & Materials Society), 2014

Monitoring of Continuous PFC Formation in Small to Moderate Size Aluminium Electrolysis Cells

Henrik Åsheim[1], Thor A. Aarhaug[2], Alain Ferber[3], Ole S. Kjos[2] and Geir M. Haarberg[1]
[1]Department of Materials Science and Engineering, NTNU; Sem Saelands vei 2, N – 7491, Trondheim, Norway
[2]SINTEF Materials and Chemistry, SINTEF; Strindveien 4, N – 7465 Trondheim, Norway
[3]SINTEF Information and Communication Technology, SINTEF; Forskningsveien 1, N – 0373, Oslo, Norway

Keywords: PFC, Anode effect, NAE-PFC, Aluminium electrolysis, GHG, Low voltage AE

Abstract

The existence of continuous or non-anode effect formed perfluorocarbons (PFC) has been documented for larger size aluminium electrolysis cells. It has been proposed that less uniformity in dissolved alumina for larger cells may elevate individual anode overvoltage sufficiently to produce PFC. Continuous PFC was monitored after the dry scrubber on a train of 28 cells at a Norwegian smelter. For this work a fourier-transform infrared spectrometer was used. Equipped with a mercury cadmium telluride detector and retrofitted with a 35 m / 11 L measurement cell it was possible to get the detection limit down in the low ppb range needed for this study.

It was discovered that also small cells could emit PFC that was not directly related to the full anode effect. Continuous formation of PFC was found to be in the form of CF_4, for the most part; however, the results indicate that C_2F_6 may also form outside the full anode effect. No numerical data for the contribution of non-anode effect emissions to the overall PFC was calculated, nonetheless, judging by the difference in intensity it will be small for this particular smelter.

Introduction and Theory

Introduction

Perflourocarbons (PFCs) are potent greenhouse gases (GHG) that are emitted from the aluminium smelters. The most common gases are tetrafluoromethane (CF_4) and hexaflouroethane (C_2F_6), but others like octafluoropropane(C_3F_8) have also been reported [1]. Common for all PFCs are their long lifetimes and very high global warming potentials, and as such, a high capacity to inflict harm on the environment. Consequently, the industry has made considerable efforts to understand the mechanism behind these unwanted emissions.

PFCs have normally been linked directly to the anode effects (AEs) and over the last 20 years the industry has made a lot of advances to reduce these emissions. The International Aluminium Institute (IAI) in London reports a decrease in PFC emissions of more than 80 % from 1990 to 2010, and has set a goal to further halve this for 2020 [2].

These achievements come as a result of introduction of new technology and serious improvements in cell control and operation. This leap forward in technology and operation also brought the means to discover emissions not directly related to the full anode effect. Studies have shown that PFC gases are also produced during electrolysis at normal cell voltages (3.7 – 4.5 V). The phenomena have been termed continuous PFC formation, or so-called low-voltage anode effects, and have been reported to occur during anode change and at the end of an underfeeding period [3]. According to Chinese data it can amount to as much as 93 % of all produced PFC [4, 5], and average 70 % [2].

The motivation of this work is to investigate if non-AE PFC is also present in smaller cells with a high kA to point-feeder ratio relative to the larger cells previously mentioned. This work has been conducted at a Norwegian smelter with pots dating from the 70s. Several changes and optimisations have naturally occurred over the years, but with a current of approximately 200 kA it is still considered small to most plants built today.

Background and principle

In a standard Hall-Heroult cell for aluminium electrowinning there are two principle reactions between carbon and alumina,

$$Al_2O_3 + 3C = 2Al + 3CO \qquad E^0 = -1.06\ V \qquad (1)$$

$$2Al_2O_3 + 3C = 4Al + 3CO_2 \qquad E^0 = -1.18\ V \qquad (2)$$

Although (1) is preferred thermodynamically, more than 90 % of the gas evolved is CO_2 resulting from the faster reaction kinetics of (2). In a typical industrial cell the current densities are about 1 A/cm^2, with an anodic overvoltage of approximately 0.5 V [6]. Close to the edges of the anodes, the current density is less than within the bulk, making the CO formation from (1) become more important [7].

When the supply of alumina to the anode decreases the potential increases through polarisation until a level where other reactions will have to occur in order for the cell to sustain the passing current. A summary of different AE studies is given by Thonstad et al. [6]. Possible reactions include the ones commonly associated with anode effect (4) and (5), but may thermodynamically also happen by the evolution of COF_2 (3), a reaction that has a potential midway between that of regular electrolysis and traditional anode effect.

$$2AlF_3 + Al_2O_3 + 3C = 4Al + 3COF_2 \qquad E^0 = -1.88\ V \qquad (3)$$

$$4AlF_3 + 3C = 4Al + 3CF_4 \qquad E^0 = -2.58\ V \qquad (4)$$

$$2AlF_3 + 2C = 2Al + C_2F_6 \qquad E^0 = -2.80\ V \qquad (5)$$

Although COF_2 could be produced electrochemically as described in (5) it is thermodynamically unstable and will decompose to CF_4 in the presence of carbon (6 – 7). In the presence of water vapour it decomposes to HF and CO_2 (8). The gas may possibly also self-decompose to CO_2 and CF_4 (9). The latter reaction is very temperature dependent and its equilibrium constant will be larger than unity below 955 °C [8].

$$2COF_2 + C = 2CO + CF_4 \qquad K = 94.8 \qquad (6)$$

$$3COF_2 + 2C = 3CO + C_2F_6 \qquad K = 5.10E{-}03 \qquad (7)$$

$$COF_2 + H_2O = 2HF + CO_2 \qquad K = 2.13E{+}09 \qquad (8)$$

$$2COF_2 = CO_2 + CF_4 \qquad K = 9.42E{-}01 \qquad (9)$$

There have been few reports of COF_2 having been chemically detected, although results from electrochemical experiments have suggested it to be present [9]. In an industrial cell this is not so strange since it reacts readily with the anode coal according to (6) or with water vapour in the off-gas stream according (8). In a lab cell on the other hand there is the possibility of strict gas control; still the presence of COF_2 is seldom reported.

However, in the past couple of years, measurements done with an open-path FTIR above an open industrial pot have shown convincing evidence that COF_2 is being produced [10]. There is less than 0.7 V difference between (2) and (3) and with anode polarisation and bubble resistance making up approximately 0.5 V, only a small potential fluctuation is needed before COF_2 could thermodynamically be produced.

Experimental

The measuring equipment was a Hartmann and Braun Bomem MB–154 Fourier Transform Infrared (FTIR) spectrometer equipped with a mercury cadmium telluride (MCT) detector for high sensitivity at a range of scanning velocities. The instrument is equipped with the infrared analysis cell 35-V-FXD-H with total volume of 11 litres and path length spanning 35 m (see Figure 1). Signal to noise can be improved with number of scans averaged, with the cost of losing gas dynamics. In the lab with a low vacuum and under optimal conditions the detection limit has been estimated to be < 100 ppt. A filter in the optical path had to be employed; otherwise the detector got fully saturated. GRAMS AI spectroscopy software [11] was used to record the spectra.

The apparatus was connected to the cumulative gas exhaust stream of 28 cells after it had passed through the dry scrubber. This minimises the need for any HF or particle filter and only Drierite® for H_2O removal was employed. Sample gas was taken from the duct at approximately 2 L/min and then through the scrubber before passing the pump, and finally into the sample cell. The cell had heating elements connected that kept the temperature at 80 °C. Measurements were conducted at resolutions of 2 and 4 cm^{-1} with an acquisition speed varying from 26 – 47 samples/min, averaged over 5 seconds in the output.

Results and Discussion

Figure 2 illustrates the part of the part of the spectrum where the PFC gases CF_4 and C_2F_6 have their most characteristic vibrational states. The spectra are taken 10 minutes apart, one during the anode effect and one slightly before. Two reference database spectra for the PFC gases overlay the anode effect signal well. The instrument was also calibrated with a 5.000 ppm CF_4 gas reference, giving a similar signal (Figure 3). From both the reference gas and the synthetic spectra generated by Spectral Calc [12] it was estimated that an absorbance of 0.035 equalled a concentration of 100 ± 5 ppb CF_4. Water would give an additional offset, but estimated to be much less than 5 ppb, especially at the interval the Drierite® was changed.

Figure 4 shows an absorbance versus time plot for CF_4, C_2F_6, SO_2 and H_2O. Two minutes into the plot a cell is being underfed and approximately 50 minutes later it goes into full anode effect with the CF_4 and C_2F_6 signals rapidly increasing. The noise around 2000 seconds is resulting from the Drierite® being changed, and as a consequence the H_2O signal nearly drops to zero.

With dry Drierite® SO_2 passes through undisturbed. There are also some peaks of C_2F_6 close to 2000 s. They are noise from the very high water signal. If C_2F_6 had been present at such large concentrations the spacious cell volume would have showed a trail of decreasing concentration.

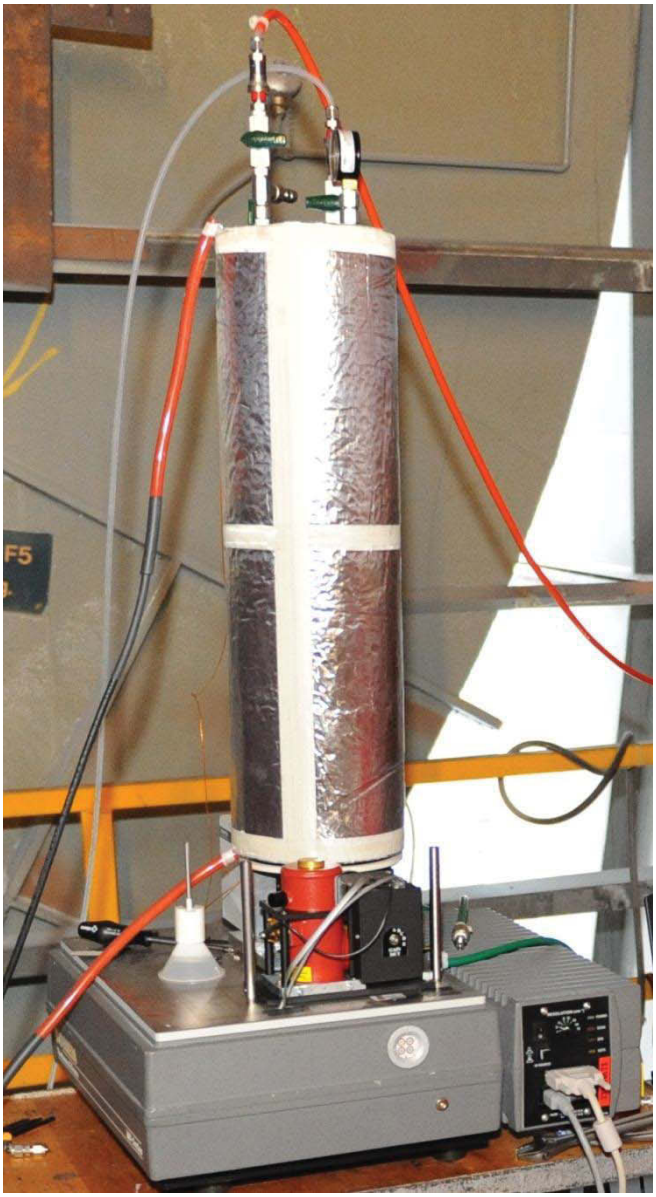

Figure 1. Apparatus setup with Bomem FTIR, a liquid N_2 cooled MCT detector and a large 11 L / 35 m cell. Two connected heat elements are covering the cell. Nitrogen is continuously flushed between the detector housings and the cell. (MCT detector housing detached in picture.)

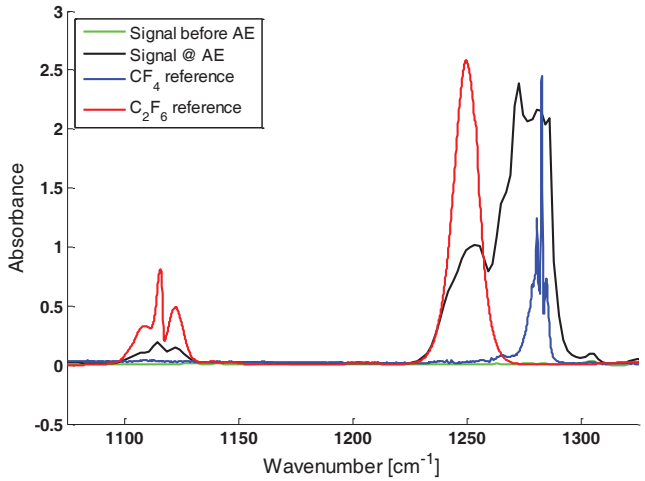

Figure 2. Reference signals from CF_4 and C_2F_6 overlaid spectra taken both before and during an anode effect.

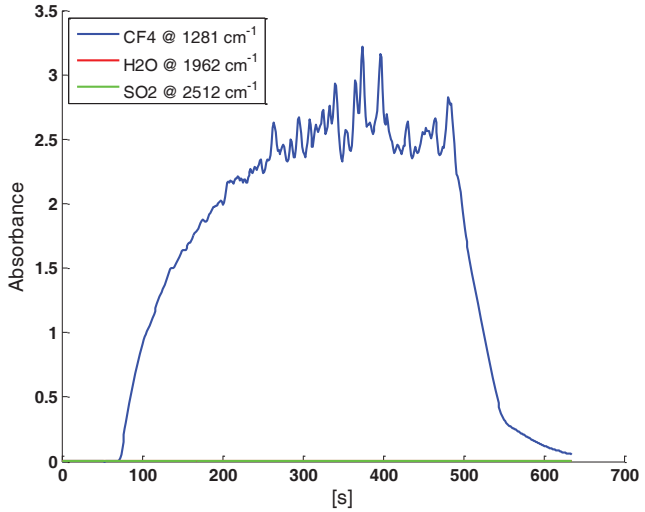

Figure 3. FTIR calibration curve for a 4.95 ppm ± 2 % CF_4 reference.

From about 400 – 1000 seconds there is a small, but broad CF_4 peak. Water has some spectral lines around 1281 cm^{-1}, but the peak shape is too dissimilar from the rising water at 1962 cm^{-1}. The peak might originate from PFC from the pot that just prior was put on underfeeding, or from any of the other 27 pots connected to the same gas duct. Interestingly, however, is that no trace of C_2F_6 is detected. During a regular anode effect the concentration of C_2F_6 is approximately 1:10 mass that of CF_4. This might stem from the fact that thermodynamically a much more negative potential is required for direct production of C_2F_6 and CF_4 through (4) and (5), than to produce COF_2 through (3) with a subsequent decomposition through (6) or (9).

A similar observation was made at the event just prior to the full anode effect of the pot at 3100 s. The event is enlarged in Figure 5 and from the enlargement it is clear that CF_4 has been increasing steadily from about 2680 s, making it a total of 7 minutes. During this period no variation in C_2F_6 was detected. Within the control instruments of the smelter a local anode effect was reported approximately 7 minutes before the full anode effect, which coincides well with the measured change in slope for CF_4 absorbance. It is possible that the cell lies in the small electrochemical window between direct CF_4 and C_2F_6 production, however, the production of CF_4 may also go by way of the intermediary COF_2.

Evidence of CF_4 being produced before the main anode effect has also been observed in the lab. Figure 6 shows mass spectrometer data obtained from an experiment conducted under potentiostatic control. Start voltage was 2.8 V vs. Al^{3+}/Al reference which was kept constant for the first 20 minutes, before being raised 0.25 V every 5 minutes.

At 45 minutes and 3.6 V the figure shows a non-negligible jump in response for mass/charge 69 (fragment CF_3^+, CF_4/C_2F_6). This response is not shared by mass 119 and as such it is safe to assume that the signal at 69 is produced only by CF_4. Not until the major anode effect at 60 minutes and 4.2 V can a change in C_2F_6 at mass 119 be observed.

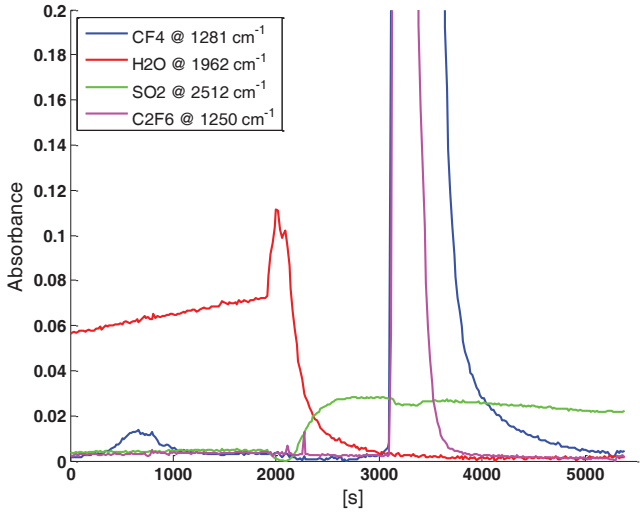

Figure 4. FTIR data for CF_4, C_2F_6, H_2O and SO_2 before and during an AE Water filter changed at 2000 s. The cell is on anode effect at 3100 s.

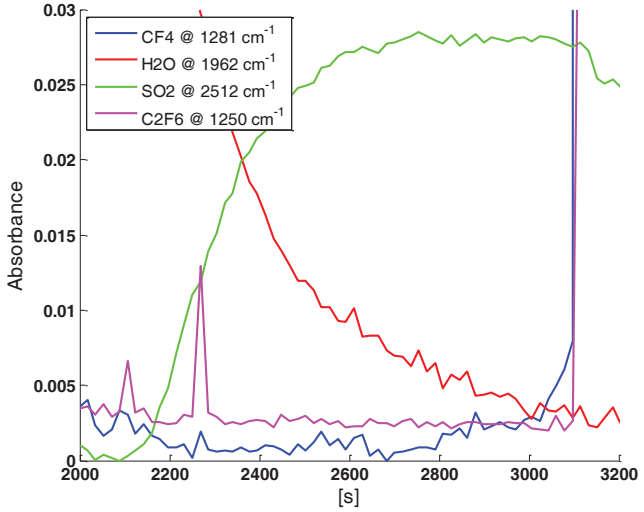

Figure 5. PFC signal from the anode effect and 10 minutes prior.

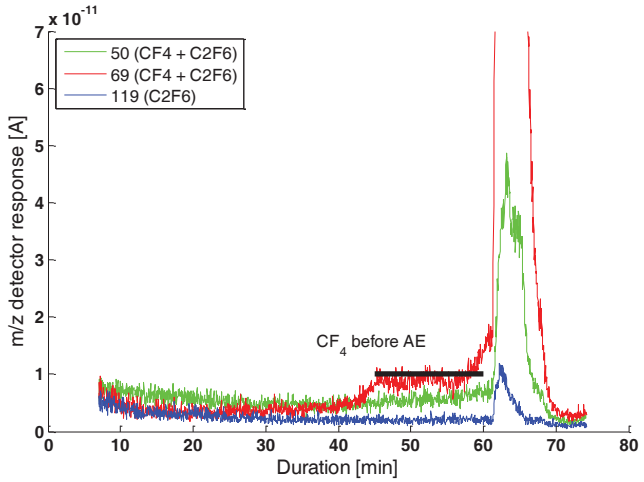

Figure 6. MS data for mass 50 (CF_4/C_2F_6), 69 (CF_4/C_2F_6) and 119 (C_2F_6).

Three cells had one out of a total of two alumina point feeders turned off to disturb the oxide balance in the bath and starve it to a level where it is just on the verge of going into an anode effect. The sequence is presented in Figure 7.

The starving began 400 seconds into the plot and the water filter was changed at 2500 s. The slight rise in PFC level up to this point is ascribed the many absorption lines of water and a couple of small water lines overlap with the main peaks of CF_4 and C_2F_6. During the next 1000 s both PFC curves rise, however, they do so in a dissimilar manner. C_2F_6 doesn't follow the ups and downs of CF_4 as in a regular anode effect. There is no doubt that CF_4 is detected, but the C_2F_6 is most likely ascribed to the filter change. On the other hand, it might also be that the rise is dampened by the falling water and that C_2F_6 is indeed produced. The amount of water would also inflict the CF_4 response, but as much more CF_4 is produced (~ 10 times during AE) any changes would be less visible. It should be clear from this that removal of water is important as it can cloud the rest of the spectra.

From 3500 s and up to 6500 s, where one of the cells went on AE, there is production of CF_4, and a mesh plot of single spectra from the region of greatest change is presented in Figure 8. In total it is almost an hour with continuous PFC emissions and Figure 8 confirms the water changes little during this time. It might come from any or several of the 28 cells, however, it is likely from one of the three starved of oxide, and most probable from the one that encountered the major anode effect at 6500 seconds. Interestingly the level of C_2F_6 remains entirely constant during this period, and as discussed earlier this could be the noise level; nonetheless it cannot be overlooked that the signal increased, noise or not, after the filter change, and a subsequent decrease down to the same level, is observed after the major anode effect. From one point of view it could look like there is a constant formation of C_2F_6 during this non-AE period.

Figure 9 shows a plot of two cells that went on anode effect only one minute apart. It is the same two cells that were set to starve in Figure 7, yet did not end up with the full AE. Three hours after starving was initiated there was a mains decoupling to connect a new cell. As soon as the power was back up the cells went on AE only a minute apart. No long period of emissions was detected in this case, possibly as a result of the power outage; although there's no guarantee there would have been one without it either.

The change in signal happens over just 150 s and is much steeper than in the previously discussed cases as well. Additionally the C_2F_6 signal changes inclination as early as CF_4, albeit to a lesser degree, which is in stark contrast to the other observed AEs where C_2F_6 only have changed abruptly just as the major AE begun. It is unclear why it looks like this. CF_4 can be argued to have a steeper slope if both cells had a relatively similar short non-AE run and the signals accumulated. C_2F_6 has previously in these results not had any stepwise increase prior to an anode effect, but the effects of tampering, both with oxide level and current, might have changed this. Possibly the oxide concentration is so badly distributed that one or more anodes are forced to an overpotential that could initiate the production of CF_4 from (4) and C_2F_6 from (5), while the rest followed regular electrolysis. Eventually this could not be sustained and a major AE was a fact.

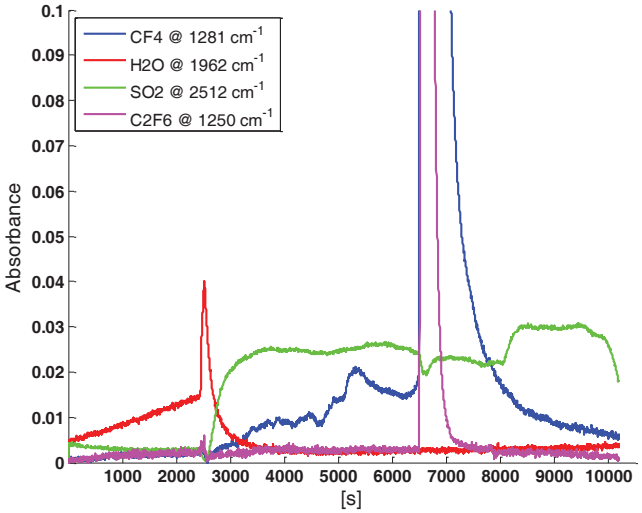

Figure 7. FTIR data for CF_4, C_2F_6, H_2O and SO_2 showing continuous PFC emissions for ~ 1 h before an anode effect. Water filter changed at 2500 s.

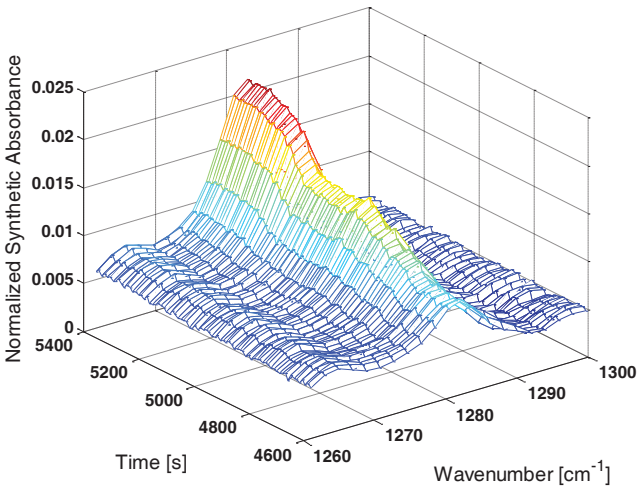

Figure 8. Mesh plot of single spectra the region of greatest change in non-AE PFC.

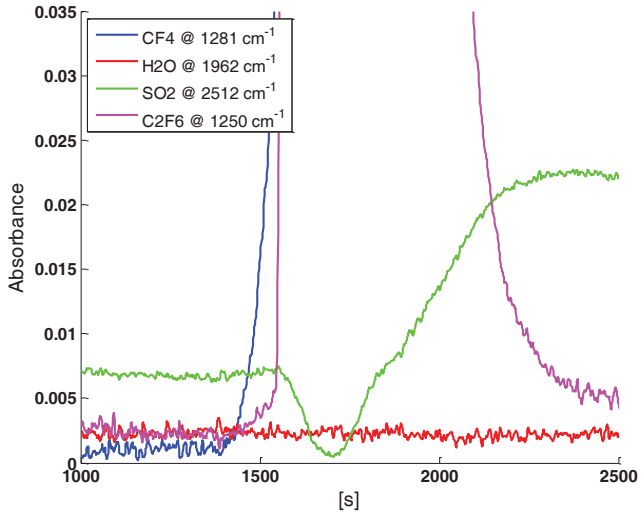

Figure 9. FTIR data for CF_4, C_2F_6, H_2O and SO_2 showing the PFC profile of two cells experiencing oxide starvation and current loss.

Figure 10 starts by showing the falling trend after the major two cell simultaneous AE. At the end of the spectra there are two similar shaped PFC peaks that might originate from an analogous event, albeit at a different magnitude. Interestingly the signal is much unlike the non-AE PFC discussed in both Figure 4 and 7. There is also some variation in the C_2F_6 response at these peaks and by looking at individual spectra it was confirmed for the top at 2800 s, any signal at 3150 is too small to be significant. At 1700 s there is also some variation in the C_2F_6 signal, with a peak value higher than that of 2800 s. In spite of that the small trail for the larger one at 1700 s suggests it has a higher character of noise than the other.

Another property of the PFC peaks at the end of the spectra is their shape. While the previous non-AE PFC curves were broad and had a low curvature, these peaks are much sharper, and have in fact a shape comparable to that of the regular AE, despite being smaller. Although no information was received from the control unit this could be an AE on the verge of happening that was fed oxide just in time – routinely or as a consequence of pot control.

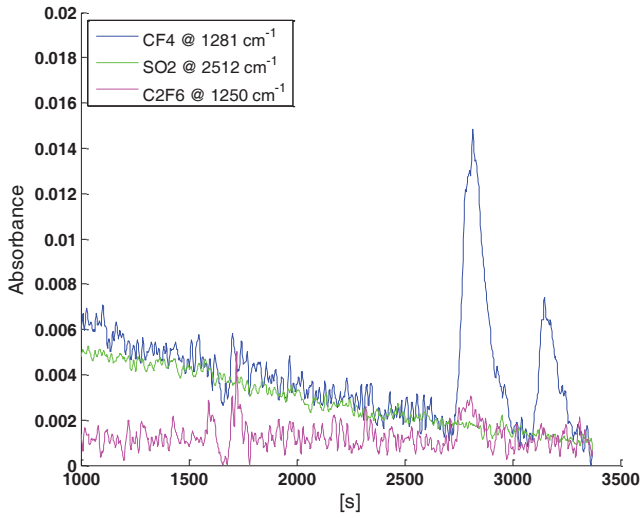

Figure 10. FTIR data for CF_4, C_2F_6, and SO_2 showing two non-AE PFC events and possible traces of C_2F_6.

Conclusions

Although most of the results related to continuous or non-AE PFC are instigated, continuous or non-AE PFC is also an attribute of smaller cells. More often than not just CF_4 is released, but as this article indicates C_2F_6 can also be formed during these events. Further investigation is needed to find the true mechanism.

Acknowledgements

This work has received financial support from The ROMA Project, Hydro and the Norwegian Research Council.

References

[1] P. Fraser, C. Trudinger, B. Dunse, P. Krummel, P. Steele, J. Mühle, P. Salameh, R. Weiss, C. Harth, A. Ganesan, R. Prinn, B. Miller, and P. Reny, "PFC emissions from Australian & global aluminium production," Boulder, Colorado, 2009.

[2] J. Marks, and C. Bayliss, "GHG Measurement and Inventory for Aluminum Production," *Light Metals 2012*, pp. 803-808: John Wiley & Sons, Inc., 2012.

[3] A. A. Zarouni, and A. A. Zarouni, "DUBAL's Experience of Low Voltage PFC Emissions," in 10th Australasian Smelting Technology Conference, Hobart, Tasmania, Australia, 2011.

[4] W. Li, Q. Zhao, S. Qiu, S. Zhang, and X. Chen, "PFC Survey in Some Smelters of China," *Light Metals 2011*, pp. 357-360: John Wiley & Sons, Inc., 2011.

[5] L. Wangxing, C. Xiping, Y. Jianhong, H. Changping, L. Yonggang, L. Defeng, and G. Huifang, "Latest Results from PFC Investigation in China," *Light Metals 2012*, pp. 617-622: John Wiley & Sons, Inc., 2012.

[6] J. Thonstad, P. Fellner, G. M. Haarberg, J. Híves, H. Kvande, and Å. Sterten, *Aluminium electrolysis / fundamentals of the Hall-Héroult process*, 3rd ed., Düsseldorf: Aluminium-Verlag, 2001.

[7] M. M. R. Dorreen, D. L. Chin, J. K. C. Lee, M. M. Hyland, and B. J. Welch, "Sulfur and Fluorine Containing Anode Gases Produced during Normal Electrolysis and Approaching an Anode Effect," *TMS Light Metals 1998*, pp. 311-316: John Wiley & Sons, Inc., 1998.

[8] O. S. Kjos, T. A. Aarhaug, E. Skybakmoen, and A. Solheim, "Studies of Perfluorocarbon Formation on Anodes in Cryolite Melts," *Light Metals 2012*, pp. 623-626: John Wiley & Sons, Inc., 2012.

[9] A. J. Calandra, C. E. Castellano, and C. M. Ferro, "Electrochemical Behavior of Different Graphite-Cryolite Alumina Melt Interfaces under Potentiodynamic Perturbations," *Electrochimica Acta,* vol. 24, no. 4, pp. 425-437, 1979.

[10] T. A. Aarhaug, "Mapping of Primary Aluminium Raw Gas Composition by Online Fourier Transform Infrared Spectroscopy," in 10th Australasian Smelting Technology Conference, Hobart, Tasmania, Australia, 2011.

[11] Thermo Scientific, "GRAMS AI Spectroscopy Software."

[12] GETS Inc., "Spectral Calc."